NONCOHERENT AND DIFFERENTIAL DETECTION OF FQPSK WITH MAXIMUM-LIKELIHOOD SEQUENCE ESTIMATION IN NONLINEAR CHANNELS

Jin-Song Lin[†]**, Kamilo Feher**
University of California, Davis
Davis, CA 95616

ABSTRACT

This paper presents noncoherent limiter-discriminator detection and differential detection of FQPSK (Feher quadrature phase-shift-keying) with maximum-likelihood sequence estimation (MLSE) techniques. Noncoherent FQPSK systems are suitable for fast fading and cochannel interference channels and channels with strong phase noise, and they can offer faster synchronization and reduce outage events compared with conventional coherent systems. In this paper, both differential detection and limiter-discriminator detection of FQPSK are discussed. We use MLSE with lookup tables to exploit the memory in noncoherently detected FQPSK signals and thus significantly improve the bit error rate (BER) performance in an additive white Gaussian noise (AWGN) channel.

KEY WORDS

Noncoherent detection, FQPSK (Feher quadrature phase-shift-keying), differential detection, limiter-discriminator (LD) detection, maximum-likelihood sequence estimation (MLSE)

INTRODUCTION

In wireless channels with large Doppler spread or fast fading ($f_D T_b > 0.01$), cochannel interference, strong phase noise, it is difficult to track the carrier frequency of the received signal correctly. To resolve this problem, noncoherent detection schemes are preferred. Noncoherent systems have faster synchronization and better performance in large Doppler spread, cochannel interference, and strong phase noise environment and can reduce burst errors and outages for relatively low data rate CDMA and TDMA (including GSM) systems [2].

FQPSK [1]-[7] is a spectrally efficient form of offset quadrature-shift-keying (OQPSK) with pulse shaping to reduce spectral sidelobes. The spectral efficiency of FQPSK can be 2 times that of

---

[†] Significant parts of this material are based on the author's reports and remain the property of the authors

Gaussian minimum-shift-keying (GMSK) and 3 times that of the pulse code modulation/frequency modulation (PCM/FM) telemetry systems [6][7]. Because of this, FQPSK could double the capacities of many currently operational nonlinearly amplified systems. The filtered version of FQPSK, or FQPSK-B, has been adopted in IRIG telemetry standard 106-00 [8] and recommended by International Consultative Committee for Space Data Systems (CCSDS) and NASA for use in high data-rate transmissions [4][9].

Noncoherent limiter-discriminator detection and differential detection of FQPSK has been proposed in [3]. In this paper, we present research that was not included in [3], including FQPSK noncoherent detection with maximum-likelihood sequence estimation (MLSE)/maximum-likelihood sequence detection (MLSD).

DIFFERENTIAL DETECTION AND LIMITER -DISCRIMINATOR DETECTION OF FQPSK

The transmitter and receiver block diagrams of differential detection and limiter-discriminator detection of FQPSK are illustrated in Figure 1 (a) - (c) [3][10].

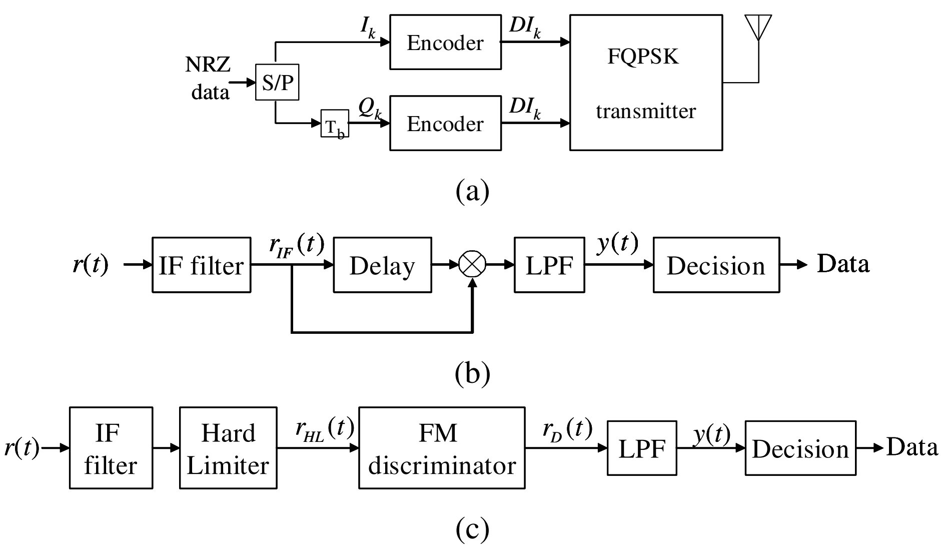

Figure 1. FQPSK noncoherent detection block diagrams. (a) Transmitter. (b) Differential detector. (c) Limiter-discriminator detector.

Figure 1 (b) illustrates the differential detection of FQPSK. It is shown in [10] that signal $y(t)$ at the output of the low pass filter in Figure 1 (b) can be written as

$$y(t) = \frac{1}{2} A(t) A(t-\tau) \cos \Delta\Phi(\tau), \qquad (1)$$

where $A(t)$ is the signal envelope after IF filter, $\Delta\Phi(\tau)$ represents the change over τ of the received signal phase plus the change in phase noise caused by the narrow-band noise.

Assume the IF bandpass filter does not distort the received signal while band-limiting the additive white Gaussian (AWGN) noise. Consider three consecutive input data, e.g., 100, 011, …, over duration $2T$. If we differentially encode the input data in transmitter so that in both I and Q channels, data "1" is mapped to a bit transition, and "0" is mapped to no bit transition, we will have a definite relationship between the NRZ input data sequence, $\Delta\Phi(2T)$, and $y(t)$, as shown in Table 1.

Data sequence input to FQPSK signal processor	Middle Bit	$\Delta\Phi(2T)$	$y(t)$
000, 101	0	0	1/2
100, 001	0	±45°	$\sqrt{2}/4$
010	1	±90°	0
110, 011	1	±135°	$-\sqrt{2}/4$
111	1	±180°	-1/2

Table 1. 2-bit differential detection of FQPSK.

From Table 1, we can see that, when the middle bit of the 3 data is 0, $y(t)$ at the output of the post-detection lowpass filter (Equation (1) with τ=$2T$) will be 1/2 or $\sqrt{2}/4$; which are larger than 0; when the middle bit is 1, $y(t)$ will be 0, $-\sqrt{2}/4$, or -1/2, which are equal to or smaller than 0. Complementary input data sequences do not produce antipodal values of $\cos\Delta\Phi(2T)$, and that results in the asymmetrical eye patterns of FQPSK after the 2-bit differential detection [10]. Therefore, if bit-by-bit threshold detection is used, a dc bias u has to be added, and the decision rule is: decide a "1" is transmitted if $y(t) > u$, and "0" otherwise. The decision scheme is illustrated in Figure 5 (a). Since the systems we discuss here are nonlinearly amplified, it is difficult, if not impossible, to find an analytical optimum value for u. In the computer simulation, the non-zero thresholds for FQPSK-B with differential detection were chosen by trial and error to minimize the required E_b/N_o for a BER of 10^{-4}.

The differential encoders in the in-phase (I) channel and the quadrature (Q) channel are:

$$DI_k = I_{k-1} \oplus DI_{k-1}, \text{ and}$$
$$DQ_k = Q_{k-1} \oplus DQ_{k-1}, \qquad (2)$$

where I_k and Q_k are the data in the I and Q channels after serial to parallel conversion, and DI_k and DQ_k are the outputs of the two differential encoders. Using Equation (2), data “1” is mapped to a bit transition and “0” is mapped to no bit transition. Figure 2 shows the result of this mapping.

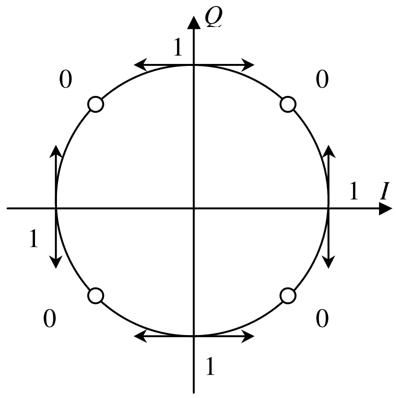

Figure 2. Illustrative phase diagram of FQPSK and the mapping result of Equation (2). After differential encoding, data “1” is mapped to a bit transition and “0” is mapped to no bit transition. Note FQPSK signal has quasi-constant envelope.

The transmitter structure of FQPSK systems with limiter-discriminator detection is the same as the one shown in Figure 1 (a). The detector is illustrated in Figure 1 (c). If the frequency discriminator is implemented by delay-and-multiply method, where the IF FM signal multiplies a replica of itself with a short delay τ and phase shift of 90°, it can be shown [10] that

$$y(t) = \frac{A^2}{2}\sin[\Delta\Phi(t)] \approx \frac{A^2}{2}[\Delta\Phi(t)] = \frac{A^2}{2}\tau\Delta f\,, \tag{3}$$

where A is the signal envelope after limiter discriminator. Figure 3 shows the FQPSK signal and its eye pattern after limiter-discriminator.

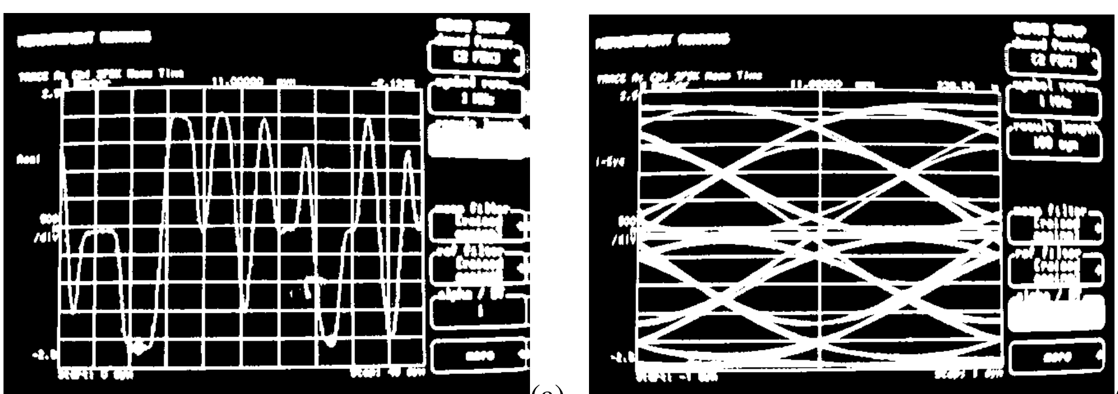
(a) (b)

Figure 3. Hardware demonstrated FQPSK-B instantaneous frequency and its eye diagram. Computer simulation resembles the measured result.

If a bit-by-bit threshold detector is used after the frequency discriminator, according to the differential encoders defined in (2), the decision rule is: decide a “1” if the magnitude of the signal at the output of the frequency discriminator is larger than a threshold v; decide a “0” otherwise. The decision criterion is illustrated in Figure 5 (b). In the computer simulation, the non-zero thresholds for FQPSK-B with limiter-discriminator detection, as in differential detection, were chosen by trial and error to minimize the required E_b/N_o for a BER of 10^{-4}.

An integrate-sample-dump (ISD) post-detection filter can be used following the frequency discriminator and lowpass filter in Figure 1 (c) to improve the BER performance. Detection decision can be made on the resulting integrated frequency, or phase. From (3), the output of the ISD filter can be written as

$$\frac{A\tau^2}{2}\int_{T_N}^{T_{N+1}} \Delta f dt = \frac{A\tau^2}{2}\left[\Phi_{N+1} - \Phi_N\right], \tag{4}$$

which is proportional to the total phase change during a bit duration. At the output of the limiter-discriminator and integrate-sample-dump post-detection filter (LD-ISD), FQPSK signals have 5-level eye diagrams, as illustrated in Figure 4. The decision rules for LD-ISD with bit-by-bit decision are similar to that of LD with bit-by-bit decision, and the only difference is the value of the thresholds.

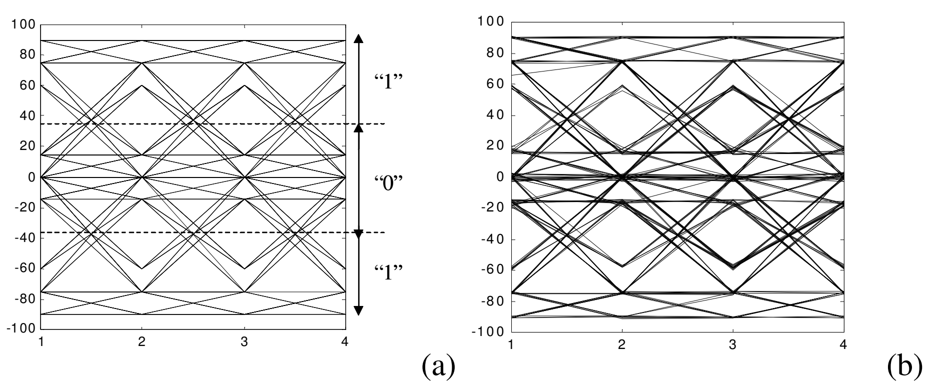

Figure 4. FQPSK signals after limiter-discriminator (LD) and integrate, sample, and dump (ISD). (a) Unfiltered FQPSK. (b) Filtered FQPSK (FQPSK-B).

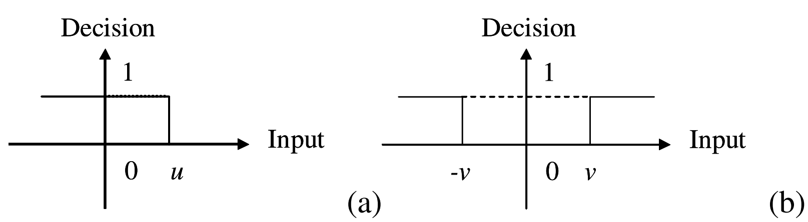

Figure 5. Decision rule for FQPSK with differential detection and discriminator detection. (a) Differential detection with bit-by-bit decision. (b) Discriminator detection with bit-by-bit decision.

MAXIMUM-LIKELIHOOD SEQUENCE ESTIMATION (MLSE): MULTI-BIT CORRELATION AND MULTI-BIT VITERBI ALGORITHM (VA)

Simon et al. [4] showed FQPSK could be interpreted as trellis coded modulation (TCM). The eye diagrams indicate clearly that FQPSK signals after differential detection or frequency discriminator detection have memory [3]. Therefore, maximum-likelihood sequence estimation [12][13] with lookup tables is considered in this paper.

Denote the total transmitted sequence as **I** and the k^{th} m-bit group of the transmitted sequence as $\mathbf{I}_k=[\, I_{mk+1}\; I_{mk+2}\; \ldots\; I_{mk+m}\,]$. In Figure 1 (b) and (c), the received signal $y(t)$ after either differential demodulation or limiter-discriminator demodulation is sampled (in the case of LD-ISD, the sampling is done with the ISD filter). Denote the total sequence of the received samples as **r** and the k^{th} m-bit group of the received samples as $\mathbf{r}_k=[\, r_{mk+1}\; r_{mk+2}\; \ldots\; r_{mk+m}\,]$. Ideally, the joint probability of **r** conditioned upon **I** is [13]

$$p(\mathbf{r} \mid \mathbf{I})=\prod_k p(\mathbf{r}_k \mid \mathbf{I}_k). \tag{5}$$

Since it could be difficult to obtain the above probability density function for a nonlinearly amplified system with non-constant envelope modulation such as FQPSK, we approximate $p(\mathbf{r} \mid \mathbf{I})$ with the joint probability of **r** conditioned upon the received samples assuming AWGN and fading are absent. Denote **u** as the total received samples when **I** is passed through a channel without AWGN and fading and then noncoherently demodulated. Let $\mathbf{u}_k=[\, u_{mk+1}\; u_{mk+2}\; \ldots\; u_{mk+m}\,]$ be the k^{th} m-bit group of **u**. **u** (including $\mathbf{u}_k$) is a nonlinear functions of **I**. Therefore, we have

$$p(\mathbf{r} \mid \mathbf{I}) \approx p(\mathbf{r} \mid \mathbf{u}(\mathbf{I}))=\prod_k p(\mathbf{r}_k \mid \mathbf{u}_k (\mathbf{I})). \tag{6}$$

Maximization of $p(\mathbf{r}_k \mid \mathbf{u}_k (\mathbf{I}))$ for each k leads to an m-bit correlation algorithm that minimizes the following Euclidean distance metrics:

$$D(\mathbf{r}_k, \mathbf{u}_k(\mathbf{I}))= \sum_{l=mk+1}^{mk+m} (r_l - u_l)^2 \,, \tag{7}$$

Therefore, maximizing $p(\mathbf{r} \mid \mathbf{u})$ is equivalent to minimizing

$$D(\mathbf{r} \mid \mathbf{u})=\sum_k D\,(\mathbf{r}_k, \mathbf{u}_k(\mathbf{I}))= \sum_k \sum_{l=mk+1}^{mk+m} (r_l - u_l)^2 \,. \tag{8}$$

In (8), the outer summation is carried out over all possible values of k. Equation (8) can be computed with an m-bit Viterbi algorithm.

Note there are 2^{m+1} instead of 2^m different possible sequences of $\mathbf{u}_k$. Because of the phase characteristics of FQPSK [3][10], depending on whether an even or odd number of 0's have been transmitted before, for any one of the 2^m possible input data sequence $\mathbf{I}_n$'s, the received sequence $\mathbf{u}_k$

will advance through a path that is symmetrical to each other, which is distinguished with superscript 0 or 1 (See Figure 6 (b)). Therefore, we have a total of 2^{m+1} different sequences of $\mathbf{u}_k$, which are denoted as $\underline{\mathbf{u}}_n=[u_{n,1}\ u_{n,2}\ \ldots\ u_{n,m}]$, $n=1,\ldots,\ 2^{m+1}$. $\underline{\mathbf{u}}_n$ is pre-stored in a lookup table $\mathbf{U}$ in the receiver. For example, for LD-ISD detection with 5-bit correlation (i.e., $m=5$), corresponding to all of the possible input data sequences $\underline{\mathbf{I}}_n$, we collect the samples (phases in degree) at the output of the ISD filter and form the following lookup table $\mathbf{U}$:

$$\text{For}\begin{bmatrix}\underline{\mathbf{I}}_1^0\\ \underline{\mathbf{I}}_2^0\\ \cdots\\ \underline{\mathbf{I}}_{2^5}^0\\ \underline{\mathbf{I}}_1^1\\ \underline{\mathbf{I}}_2^1\\ \cdots\\ \underline{\mathbf{I}}_{2^5}^1\end{bmatrix}=\begin{bmatrix}00000\\00001\\ \cdots\\11111\\00000\\00001\\ \cdots\\11111\end{bmatrix},\ \mathbf{U}=\begin{bmatrix}\underline{\mathbf{u}}_1^0\\ \underline{\mathbf{u}}_2^0\\ \cdots\\ \underline{\mathbf{u}}_{2^5}^0\\ \underline{\mathbf{u}}_1^1\\ \underline{\mathbf{u}}_2^1\\ \cdots\\ \underline{\mathbf{u}}_{2^5}^1\end{bmatrix}=\begin{bmatrix}3.8&0.0&0.0&0.0&-5.6\\3.5&0.0&0.0&14.4&64.6\\ &&\cdots&&\\79.8&90.0&90.0&90.0&79.5\\-3.8&0.0&0.0&0.0&5.6\\-3.5&0.0&0.0&-14.4&-64.6\\ &&\cdots&&\\-79.8&-90.0&-90.0&-90.0&-79.5\end{bmatrix}.$$

Note $\mathbf{U}$ is generated in a noiseless channel without fading, and averaging is needed to obtain $\underline{\mathbf{u}}_n$.

MLSE with Multi-bit Correlation Detector

The multi-bit correlation detector then correlates $\mathbf{r}_k$ that falls in an m-bit sliding window with each $\underline{\mathbf{u}}_n$ ($n=1,\ldots,\ 2^{m+1}$) and finds the $\underline{\mathbf{I}}_n$ which minimizes the Euclidean distance metric $D(\mathbf{r}_k, \underline{\mathbf{u}}_n(\underline{\mathbf{I}}_n))$, i.e.:

$$\hat{\underline{\mathbf{I}}}_k=\arg\min_{\underline{\mathbf{I}}_n}\left[D\left(\mathbf{r}_k,\underline{\mathbf{u}}_n\left(\underline{\mathbf{I}}_n\right)\right)\right]=\arg\min_{\underline{\mathbf{I}}_n}\left[\sum_{l=mk+1}^{mk+m}(r_l-u_{n,l})^2\right],\qquad n=1,\ldots,2^{m+1}\tag{9}$$

At last, $\hat{\underline{\mathbf{I}}}_k$ ($k=1, 2,\ldots$) are combined to form the final estimate of the transmitted signal.

MLSE with Multi-bit Viterbi Algorithm (VA)

The minimization of (8) can be carried out by an m-bit Viterbi algorithm that is illustrated in Figure 6 (a). Denote the n^{th} state of the 2^{m+1} possible states as $\mathbf{s}_n=[I_{n,1}\ I_{n,2}\ \ldots\ I_{n,m}]^{ind}$, $n = 1, 2, \ldots, 2^{m+1}$. The state transition diagram is illustrated in Figure 6 (b).

The n^{th} row of the lookup table $\mathbf{U}$ (or $\underline{\mathbf{u}}_n$) corresponds to the state $\mathbf{s}_n$. The initial distance metric for the state $\mathbf{s}_n$ is

$$DM_{n,1}\left(\underline{\mathbf{I}}_1\right)=\sum_{l=1}^{m}(r_l-u_{n,l})^2,\ \ n = 1, 2, \ldots, 2^{m+1},\tag{10}$$

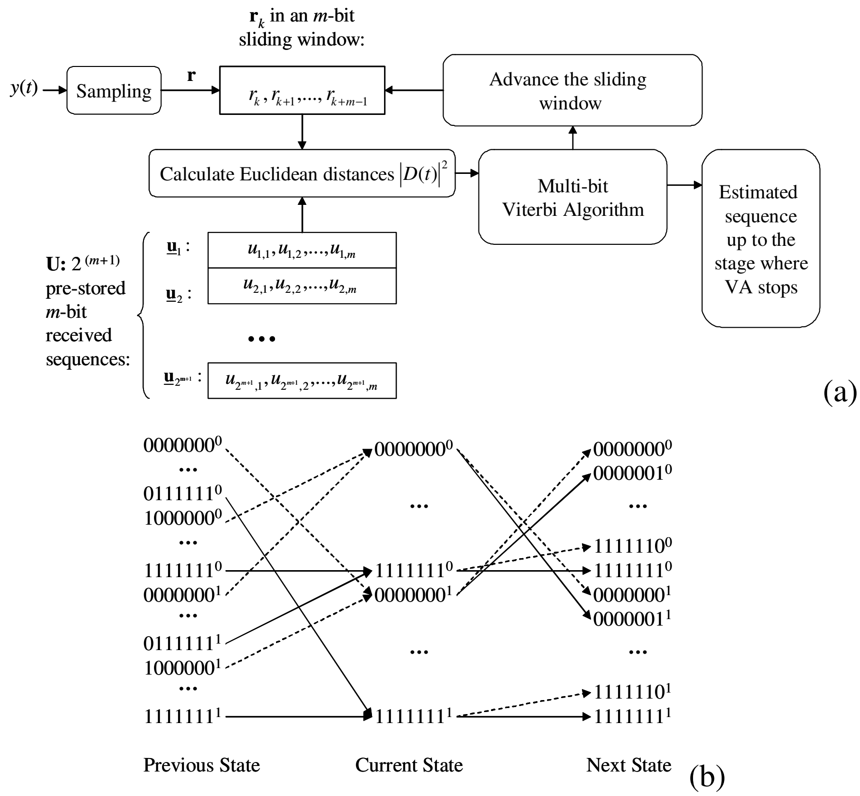

Figure 6. Maximum-likelihood sequence estimation (MLSE) used in noncoherent detection of FQPSK. (a) Multi-bit Viterbi algorithm detector. $y(t)$ is the output of the noncoherent demodulator in Figure. 1. (b) State transition diagram of the 7-bit Viterbi algorithm.

where $u_{n,l}$ is the $(n,l)^{\text{th}}$ element of $\mathbf{U}$. The accumulated metric of the state $\mathbf{s}_{\mathrm{n}}$ at stage k is

$$DM_{n,k}(\underline{\mathbf{I}}_k) = \min_{n-}\left[DM_{n-,k-1}(\underline{\mathbf{I}}_{k-1})\right] + D(\mathbf{r}_k, \underline{\mathbf{u}}_n), \; n = 1, 2, \ldots, 2^{m+1}, \tag{11}$$

where $DM_{n,k}(\underline{\mathbf{I}}_k)$ is the metric corresponding to the surviving path of state $\mathbf{s}_{\mathrm{n}}$ up to the stage k, $\min_{n-}\left[DM_{n-,k-1}(\underline{\mathbf{I}}_{k-1})\right]$ is the minimum of the accumulated metrics of the two preceding states of state $\mathbf{s}_{\mathrm{n}}$, and $D(\mathbf{r}_k, \underline{\mathbf{u}}_n)$ is the Euclidean distance between $\mathbf{r}_k$ and the pre-stored m-bit sequence $\underline{\mathbf{u}}_n$.

COMPUTATIONAL RESULTS

Figure 7 (a) illustrates the BER performance of nonlinearly amplified FQPSK-B systems with differential detection (DD) in a stationary AWGN channel. At BER= 10^{-4} , FQPSK differential detectors with primitive bit-by-bit sample-and-hold (S&H) threshold detection require E_b/N_o of about 22 dB, which is not realistic in practical applications. With multi-bit correlation, the differential detectors of FQPSK-B show 5 dB improvement.

BER performance of nonlinearly amplified FQPSK-B with limiter-discriminator (LD) detection in a stationary AWGN channel is illustrated in Figure 7 (b). For BER $=10^{-4}$, with multi-bit correlation, the limiter-discriminator detectors of FQPSK-B show 4 dB improvement over bit-by-bit threshold detectors. With a multi-bit detector using Viterbi algorithm, the required E_b/N_o are reduced by 2 dB to 12.9 dB. For FQPSK, discriminator detection is superior to differential detection in AWGN channels, although this is not true in all circumstances [14].

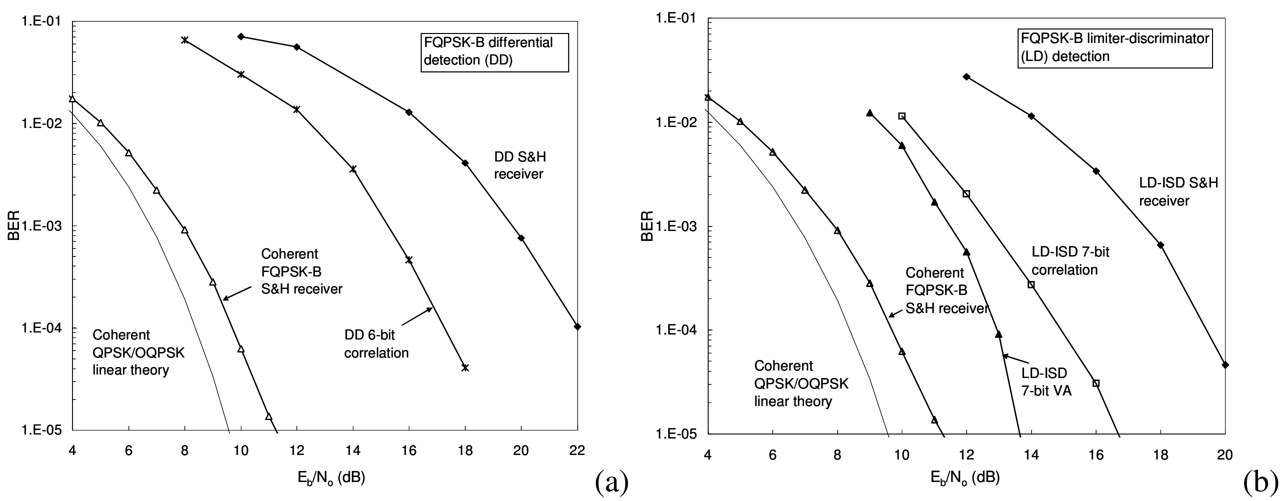

Figure 7. Bit error rate (BER) performance of noncoherent detection of nonlinearly amplified FQPSK. (a) FQPSK with differential detection (DD). (b) FQPSK with discriminator detection with ISD filter (LD-ISD).

CONCLUSIONS

We have presented noncoherent detection of nonlinearly amplified spectrum efficient FQPSK systems with MLSD and diversity. To exploit the inherent memory in noncoherently detected FQPSK signals, we have applied the multi-bit correlation algorithm and multi-bit Viterbi algorithm for FQPSK noncoherent systems. We have shown that, with multi-bit correlation, the BER performance of both differential detection and limiter-discriminator detection of FQPSK can be improved in terms of the required E_b/N_o by 4-5 dB over that of bit-by-bit S&H threshold detection; with a multi-bit Viterbi algorithm, the BER performance can be further improved by 2 dB. The techniques we propose in this paper could be applied to other offset-keyed modulation systems such as OQPSK and spectrum efficient shaped offset QPSK (SOQPSK) systems [4]

ACKNOWLEDGMENT

J.-S. L. would like to thank Prof. Soo-Young Chang of University of Suwon, Korea and Prof. Zhi Ding of University of California, Davis for their valuable comments and suggestions.

REFERENCES

[1] K. Feher, et al.: US Patents 4,567,602; 4,644,565; 5,491,457; 5,784,402, and 6,198,777.

[2] K. Feher, Wireless Digital Communications: Modulation and Spread Spectrum Applications, New Jersey, Prentice Hall, 1995.

[3] J.-S. Lin, K. Feher: "Fast Synchronized Noncoherent Detection of Standardized FQPSK and OQPSK," Proceeding of European Telemetering Conference, May 2002

[4] M. K. Simon, Bandwidth-Efficient Digital Modulation with Application to Deep-Space Communications, Monograph 3, Deep-Space Communications and Navigation Series, Jet Propulsion Laboratory Publication 00-17, June 2001.

[5] S. Kato, and K. Feher, "XPSK: A New Cross-correlated Phase-Shift Keying Modulation Technique", IEEE Trans. Commun., vol. 31, No. 5, May 1983.

[6] K. Feher, "FQPSK Transceivers Double the Spectral Efficiency of Wireless and Telemetry Systems," Applied Microwave & Wireless, June 1998.

[7] J.-S. Lin, K. Feher, "Bandwidth Efficiency and BER Performance of Non-linearly Amplified Enhanced and FEC Coded FQPSK," Proceeding of International Telemetering Conference, Las Vegas, NV, October 23-26, 2000.

[8] Telemetry Group, Range Commanders Council, Telemetry Standards. IRIG Standard 106-00, Secretariat, Range Commanders Council, U.S. army White Sands Missile Range, New Mexico 88002-5110, January 2000.

[9] CCSDS 401.0-B BLUE BOOK, Recommendations for Space Data Systems Standards, Consultative Committee for Space Data Systems, June 2001

[10] J.-S. Lin, K. Feher, "Noncoherent Detection of Standardized FQPSK and OQPSK in Nonlinear Channels," unpublished.

[11] M. K. Simon, and C. C.Wang, "Differential Detection of Gaussian MSK in a Mobile Radio Environment", IEEE Trans. Veh. Technol., vol. 33, No. 4, November, 1984, pp. 307-320.

[12] K. Ohno, and F. Adachi, "Performance Evaluation of Various Decision Schemes For Frequency Demodulation of Narrowband Digital FM Signals In Land Mobile Radio Channels", IEEE Trans. Veh. Technol., 1990, vol. 39, pp. 109-116.

[13] D. Divsalar, M. K. Simon, "Maximum-Likelihood Differential Detection Of Uncoded And Trellis Coded Amplitude Phase Modulation Over AWGN And Fading Channels-Metrics And Performance," IEEE Trans. Commun., vol. 42, No. 1, January 1994.

[14] K. Hirade, "Mobile-Radio Communications," Advanced Digital Communications: Systems and Signal Processing Techniques, K. Feher, editor. Englewood Cliffs, N.J.: Prentice-Hall, c1987. pp. 509-528.